Supplement of Atmos. Chem. Phys., 19, 7397–7408, 2019
https://doi.org/10.5194/acp-19-7397-2019-supplement

Atmospheric Chemistry and Physics
Open Access
EGU

Supplement of

Direct radiative effect of dust–pollution interactions

Klaus Klingmüller et al.

Correspondence to: Klaus Klingmüller (k.klingmueller@mpic.de)

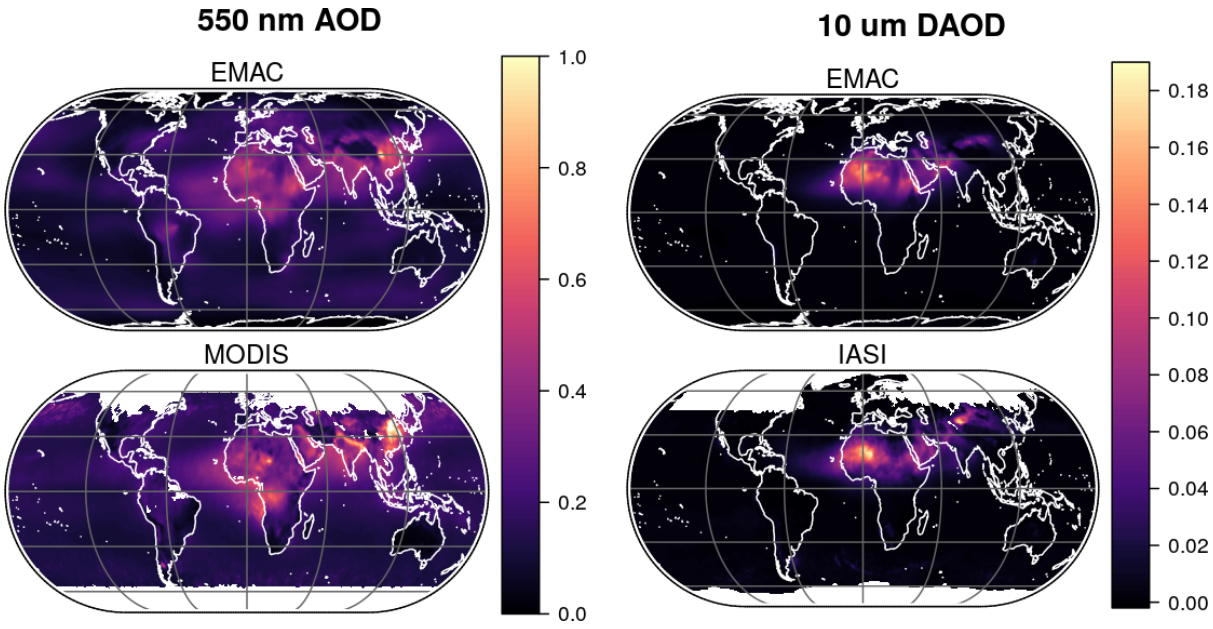

Figure S1: The EMAC setup yields realistic results for the AOD at visible wavelength (550 nm, left) and in the infrared (10 μm, right, dust related AOD only). The top row shows the model results, the bottom row satellite observations by MODIS (left) and IASI (right).

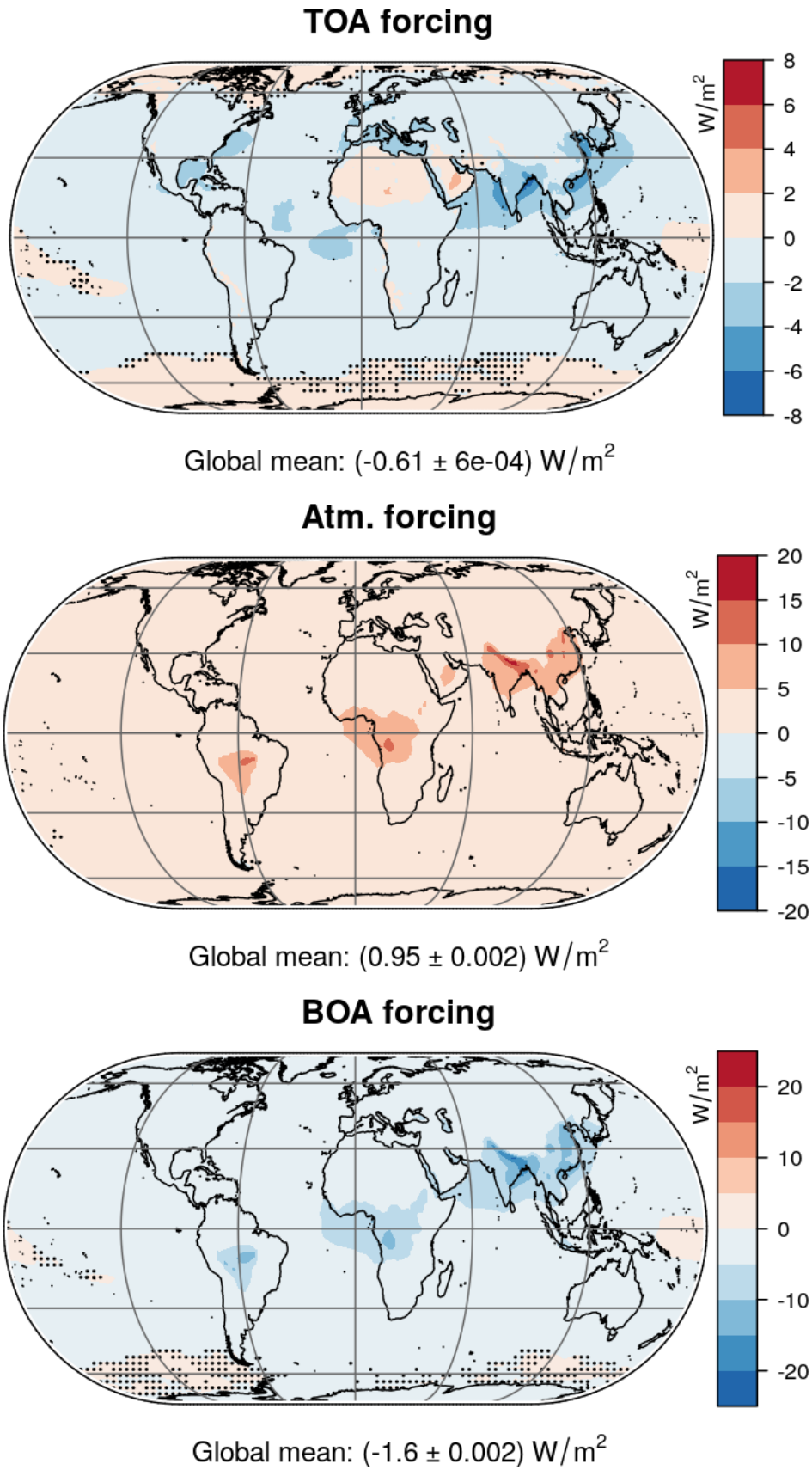

Figure S2: The total (solar and terrestrial) direct radiative forcing of anthropogenic aerosol in the dust free scenario at the top of the atmosphere (TOA, top), within the atmosphere (centre) and at the bottom of the atmosphere (BOA, bottom). Dots indicate regions where the forcing is insignificant.

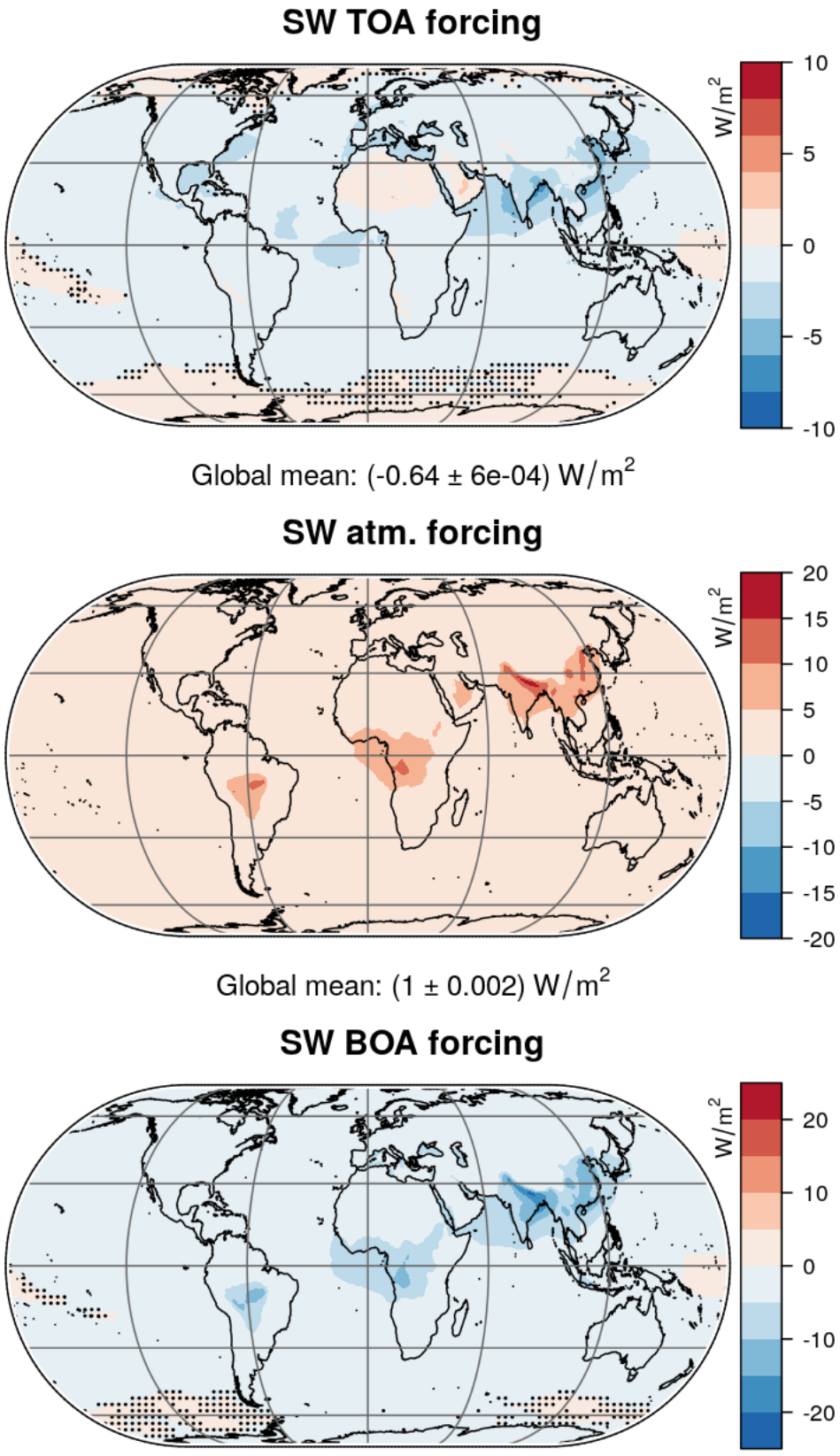

Figure S3: Same as Fig. S2, but only considering solar (shortwave, SW) radiation.

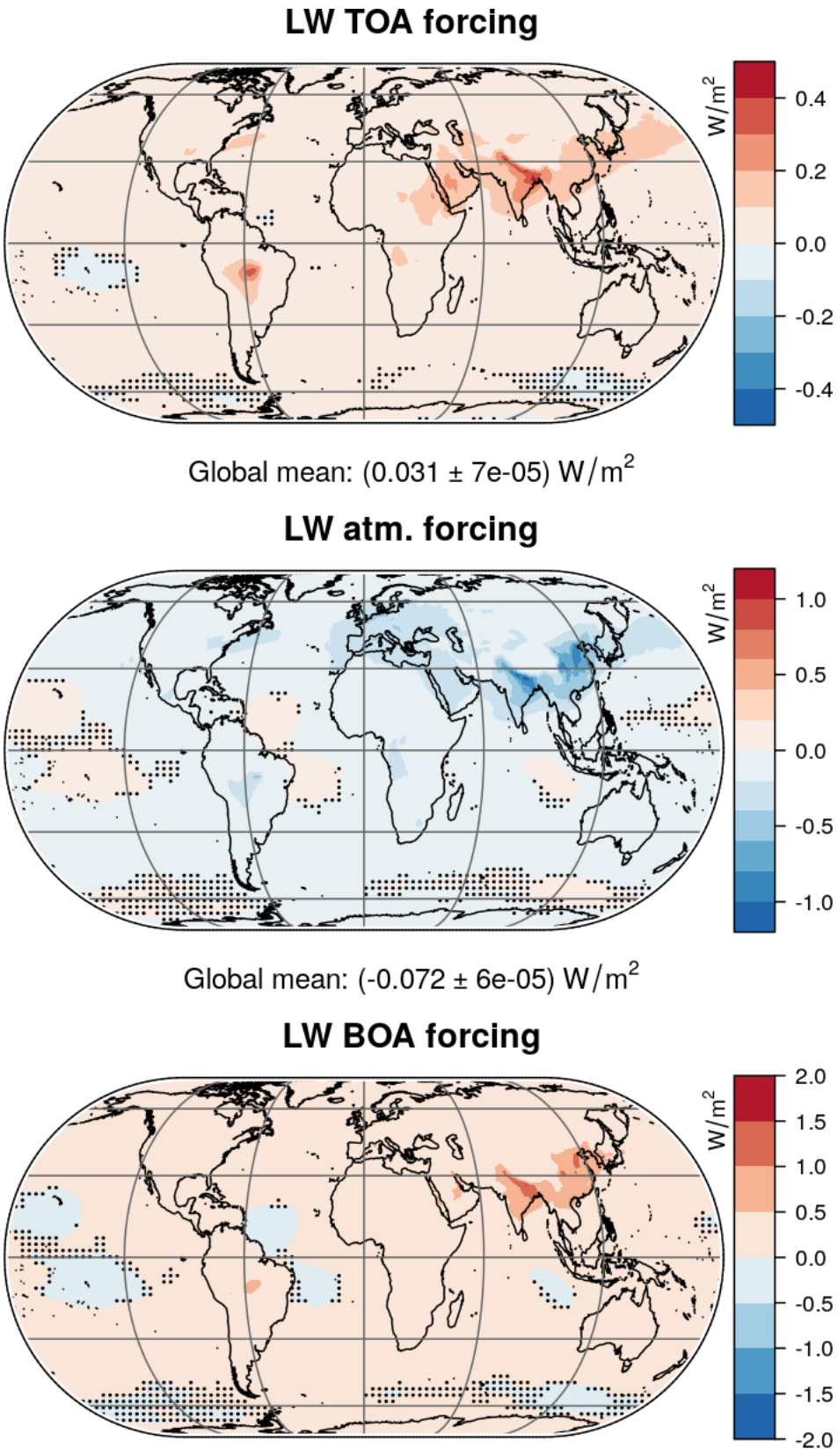

Figure S4: Same as Fig. S2, but only considering terrestrial (longwave, LW) radiation.

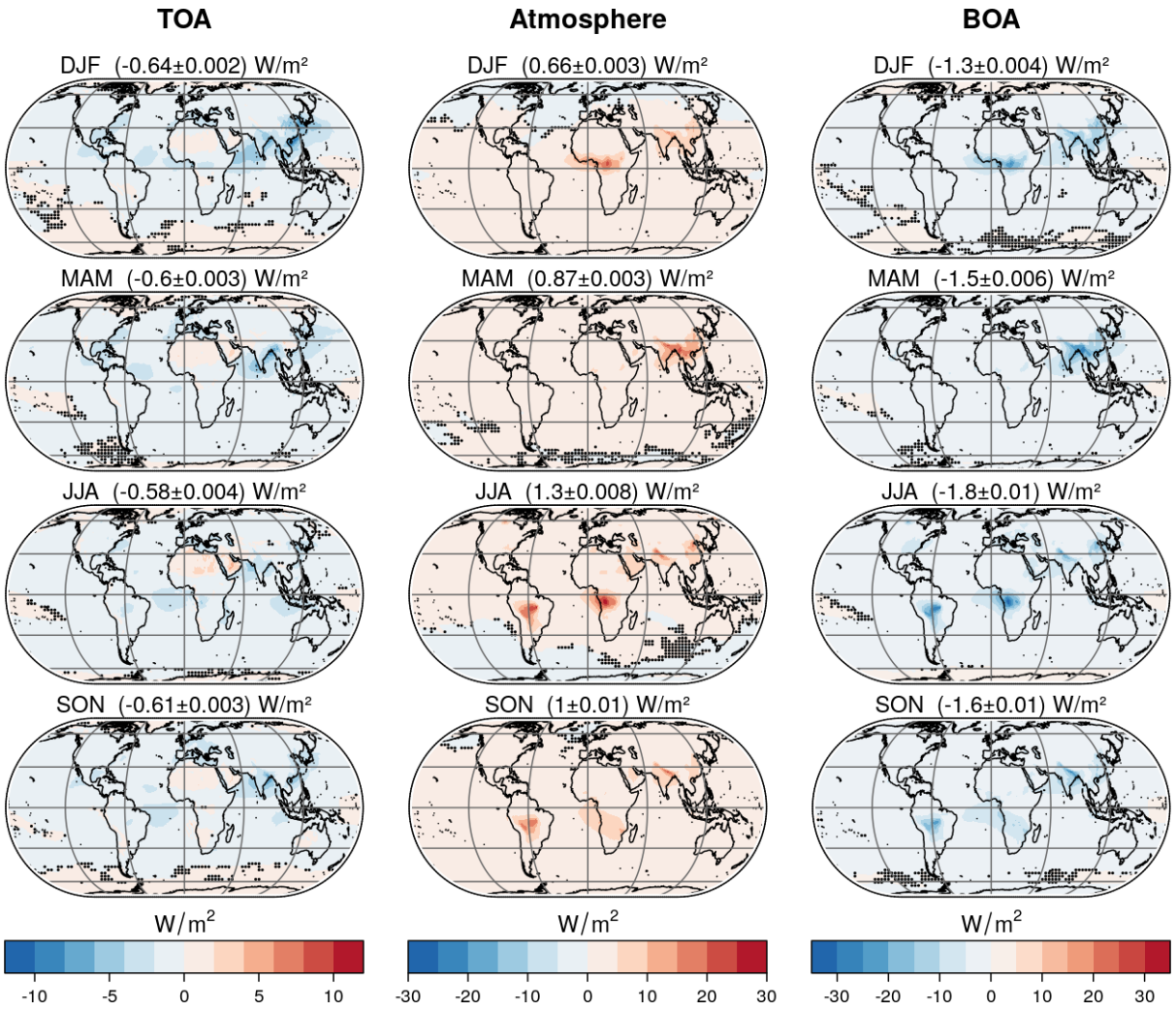

Figure S5: Same as Fig. S2, but for each season (December, January, February (DJF); March, April, May (MAM); June, July, August (JJA); September, October, November (SON)) individually.

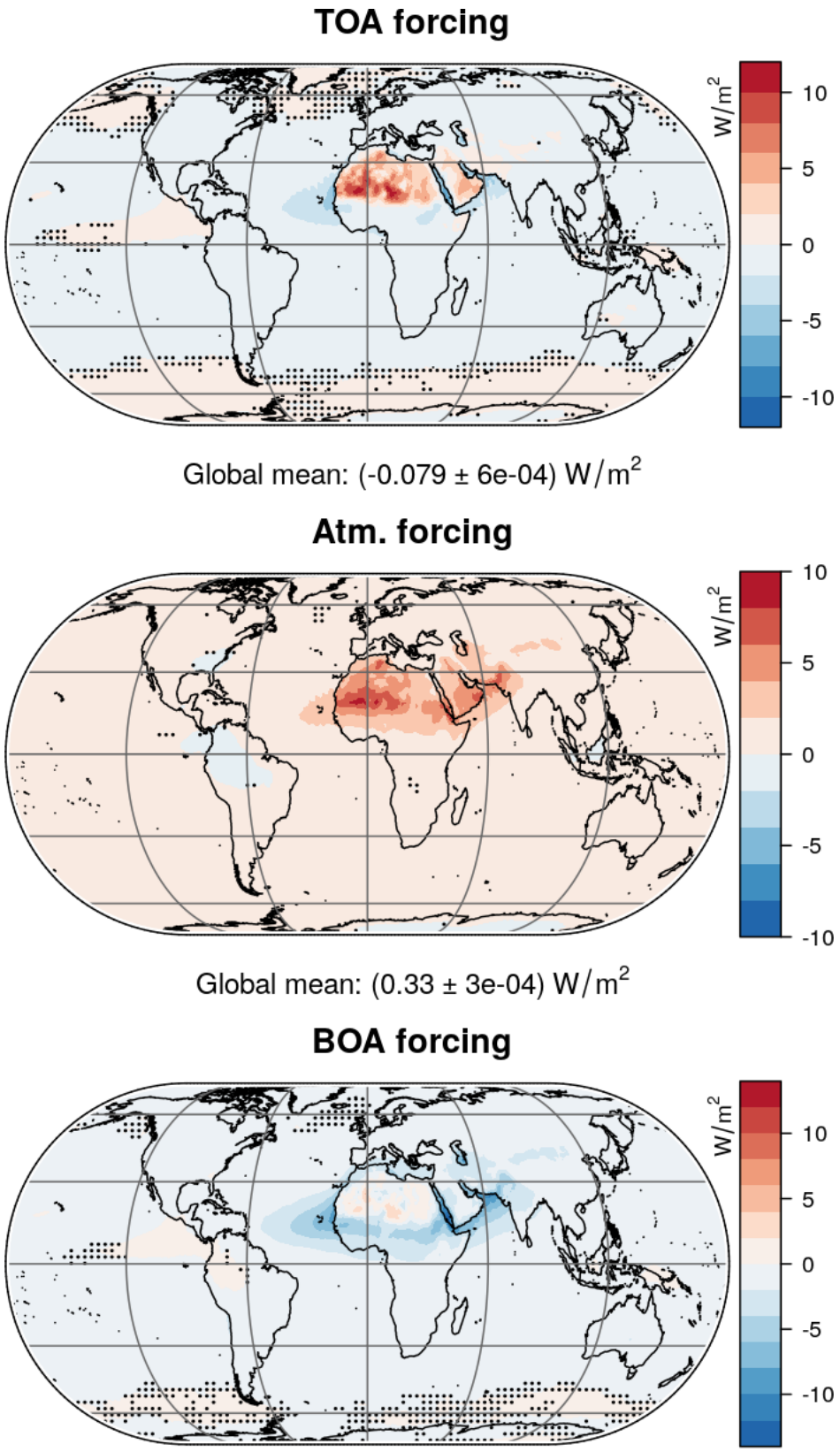

Figure S6: The total (solar and terrestrial) direct radiative forcing of mineral dust in the natural scenario at the top of the atmosphere (TOA, top), within the atmosphere (centre) and at the bottom of the atmosphere (BOA, bottom). Dots indicate regions where the forcing is insignificant.

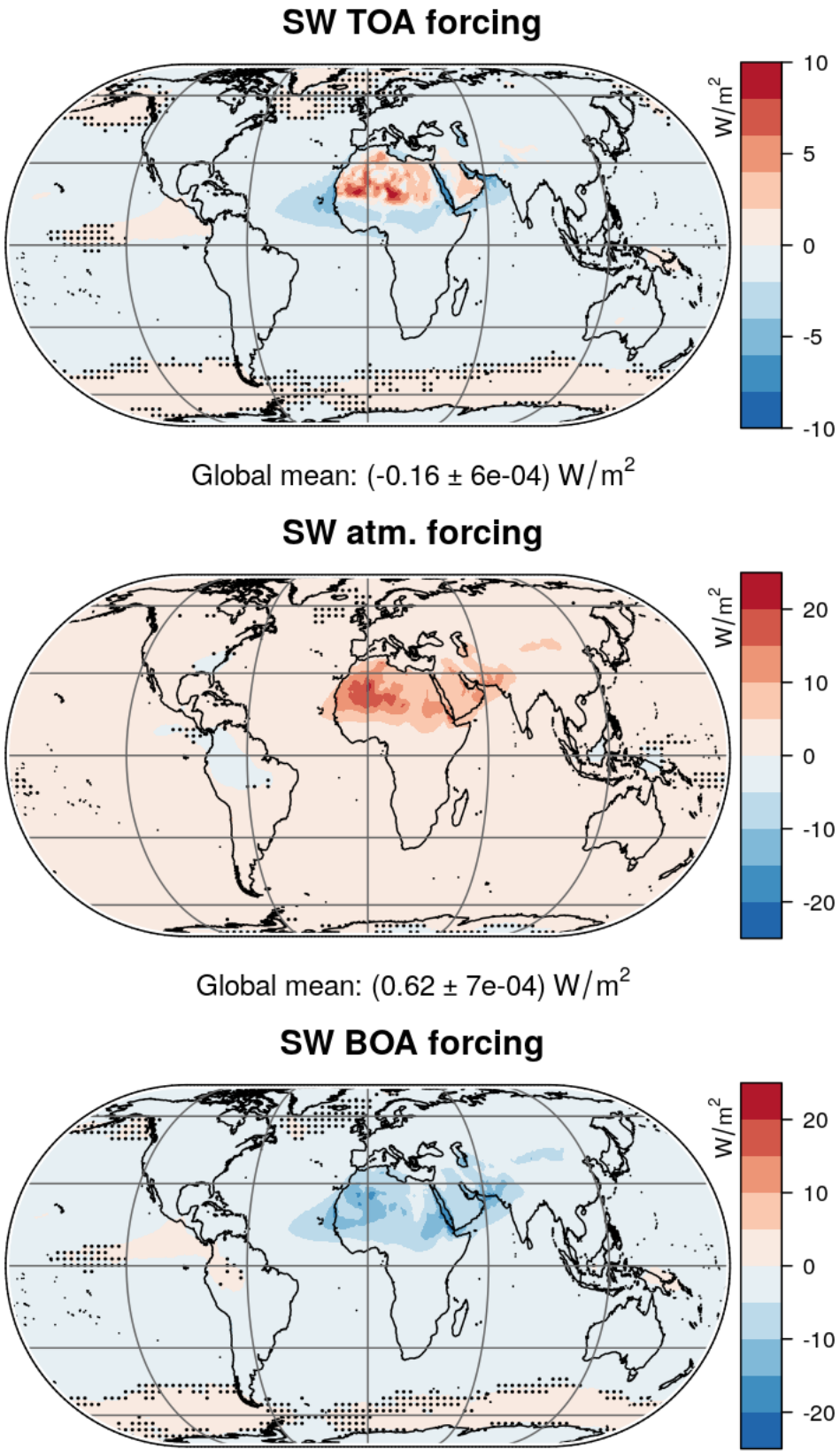

Figure S7: Same as Fig. S6, but only considering solar (shortwave, SW) radiation.

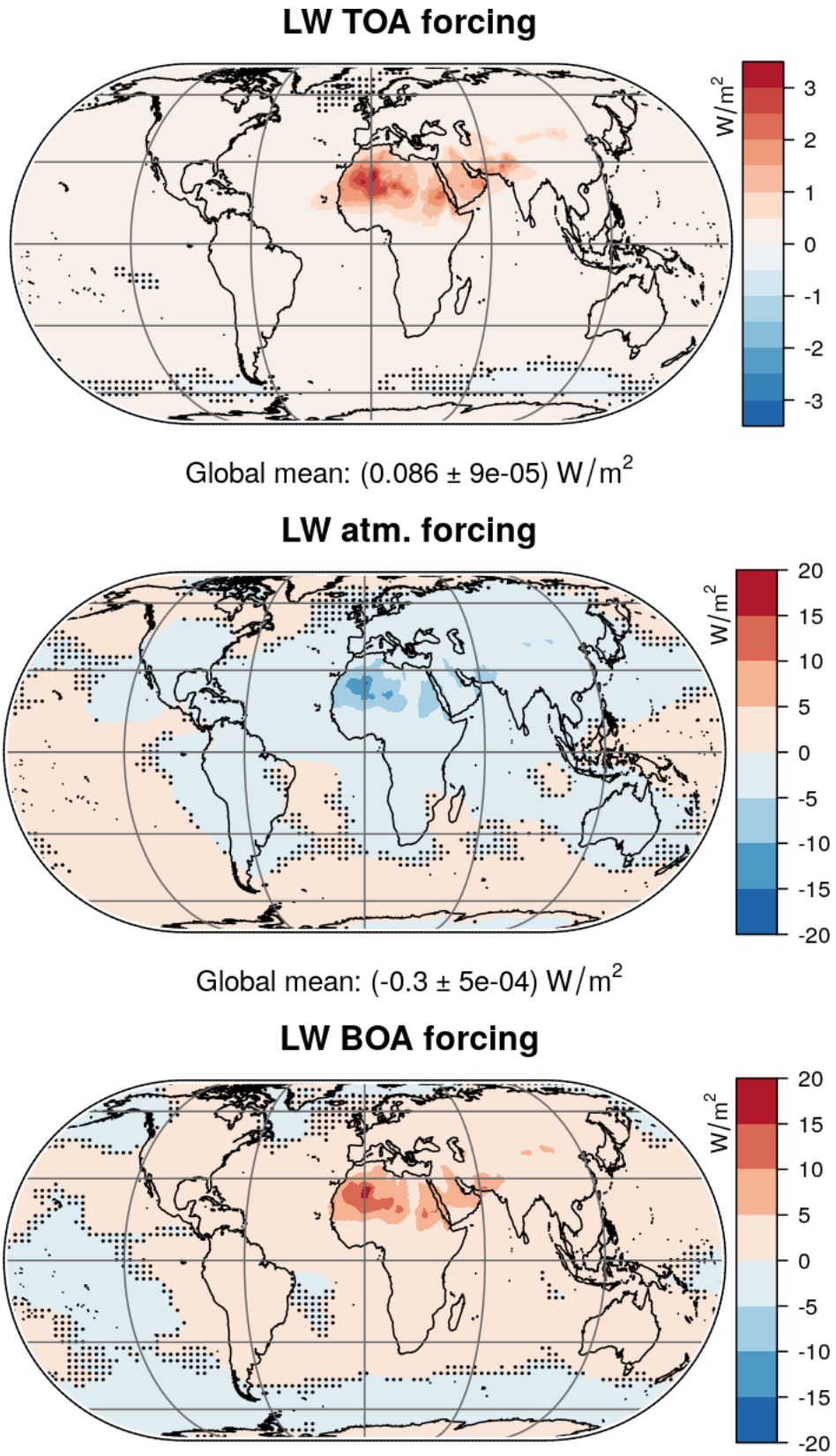

Figure S8: Same as Fig. S6, but only considering terrestrial (longwave, LW) radiation.

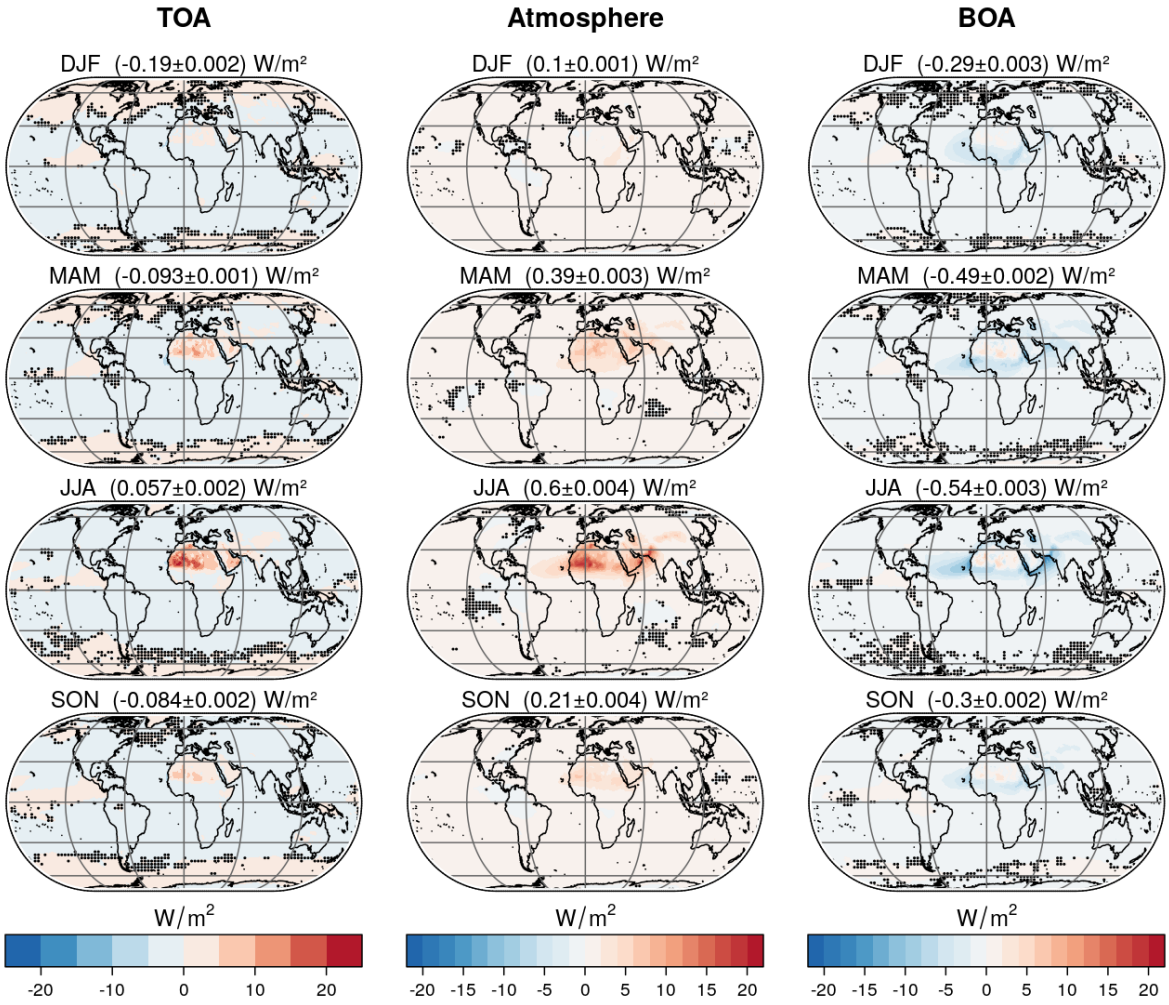

Figure S9: Same as Fig. S6, but for each season (December, January, February (DJF); March, April, May (MAM); June, July, August (JJA); September, October, November (SON)) individually.

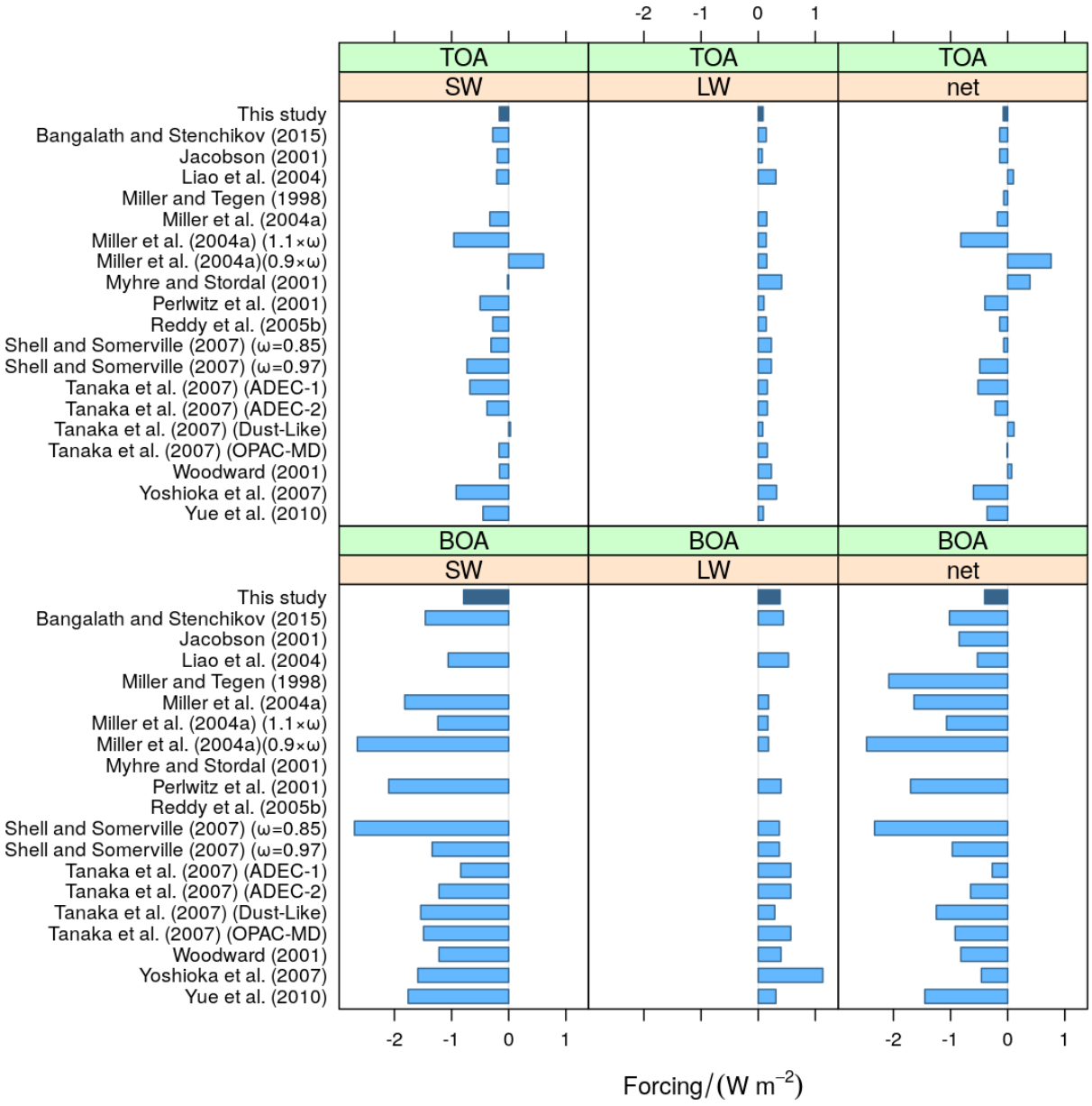

Figure S10: Global direct radiative forcing by dust in the EMAC simulations of the present study in comparison to results of previous studies (Yue et al. 2010, Table 1).

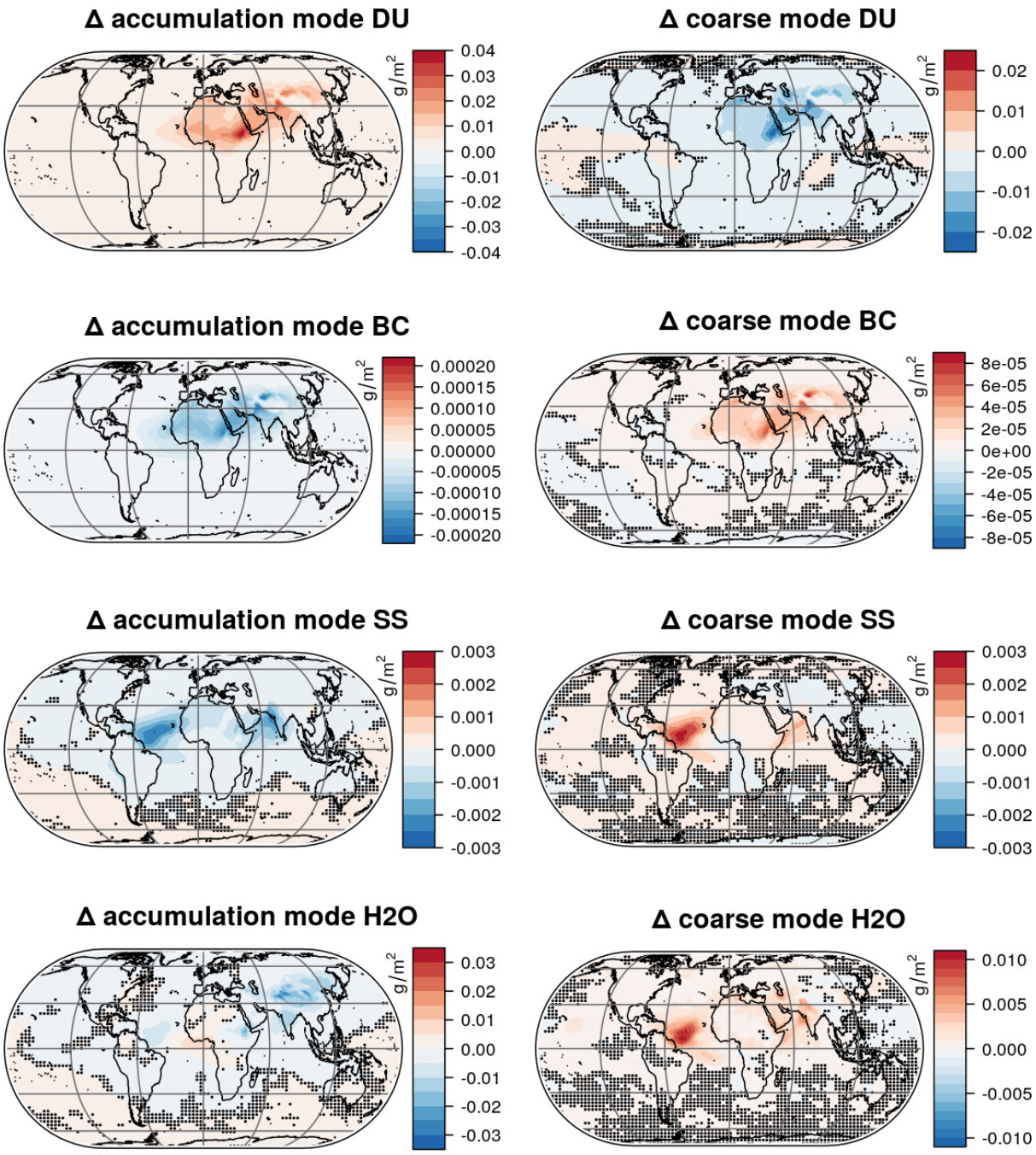

Figure S11: Effect of the dust-pollution interactions on the burdens of major aerosol components (left column: accumulation mode, right column: coarse mode).

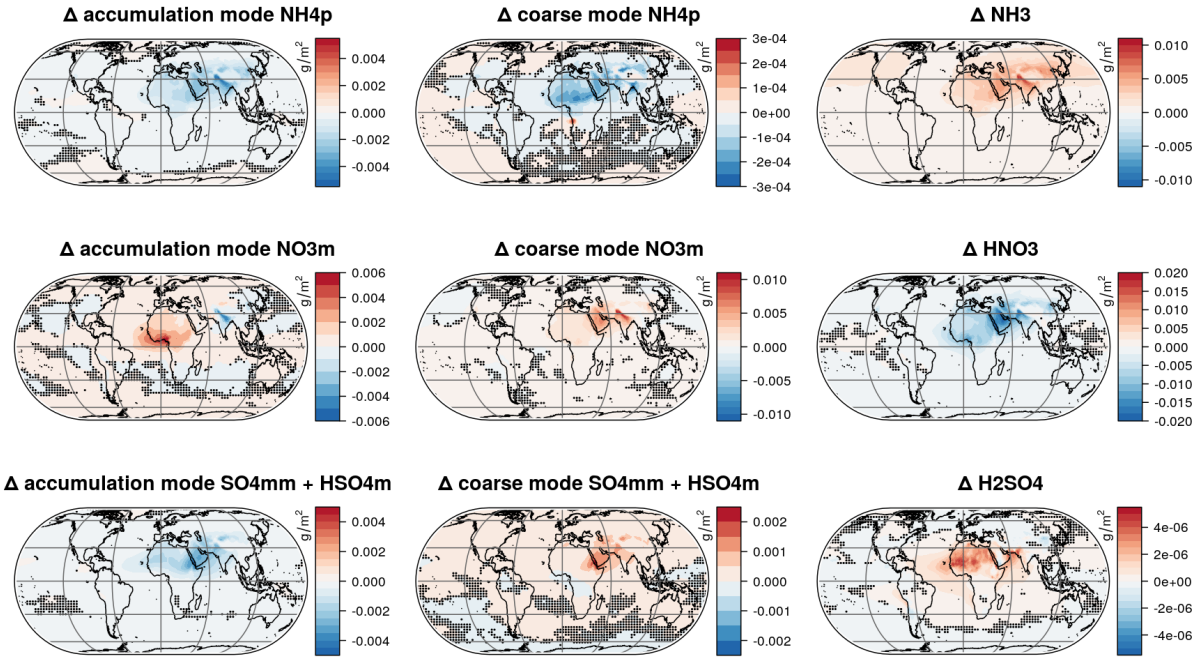

Figure S12: Effect of the dust-pollution interactions on the burdens of the main aerosol ions (left column: accumulation mode, centre column: coarse mode) and the corresponding precursor gases (right column).

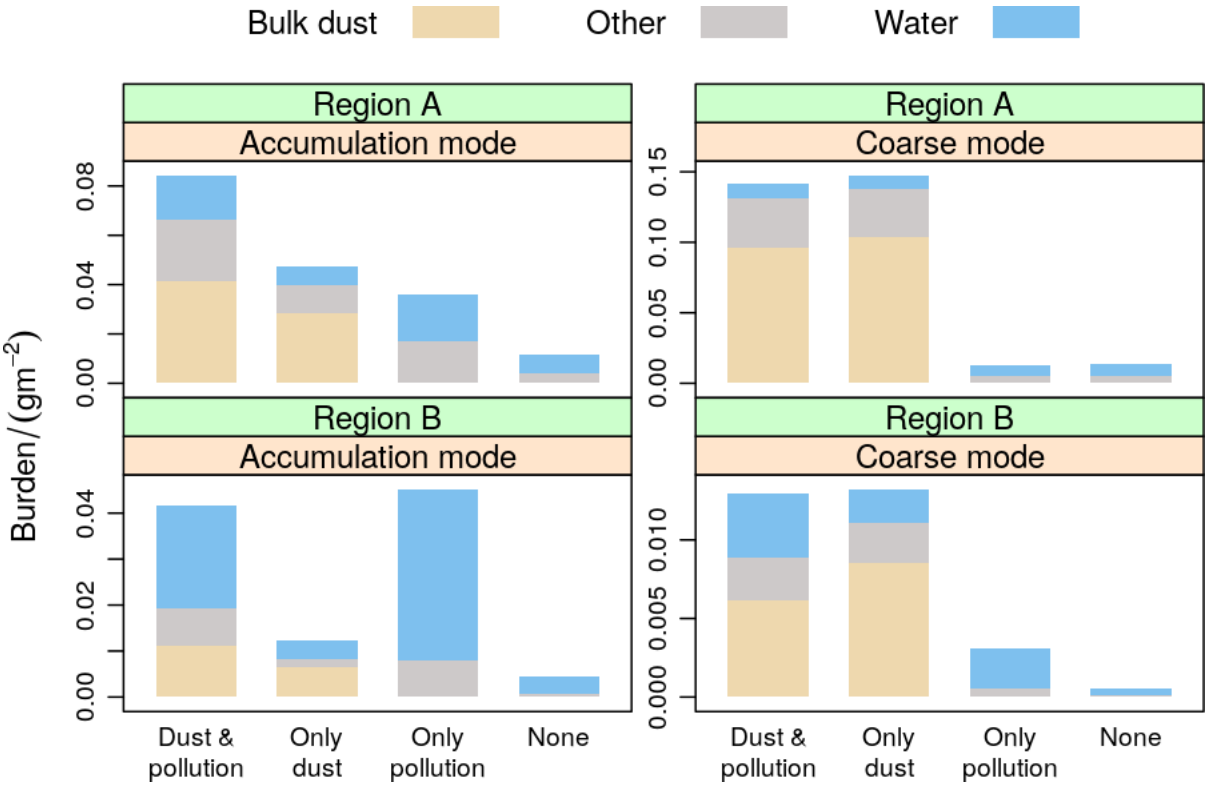

Figure S13: Annual mean aerosol mass burdens over regions A (top) and B (bottom) in Fig. 1 for each of the four simulations individually.

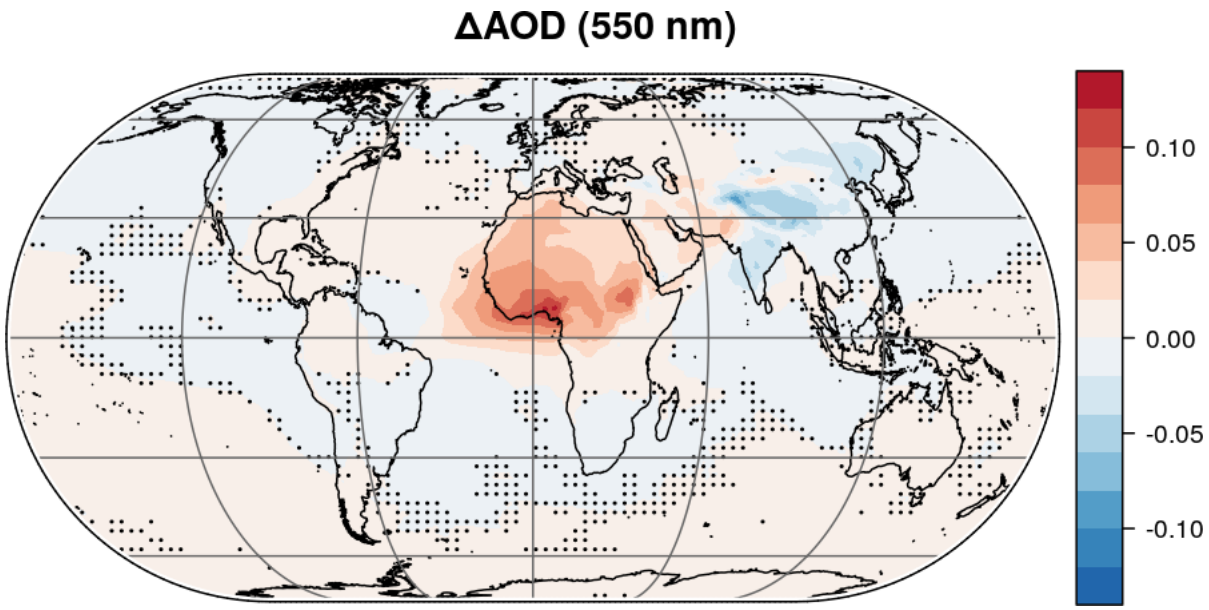

Figure S14: Same as Fig. 3 (top) but at 550 nm wavelength.

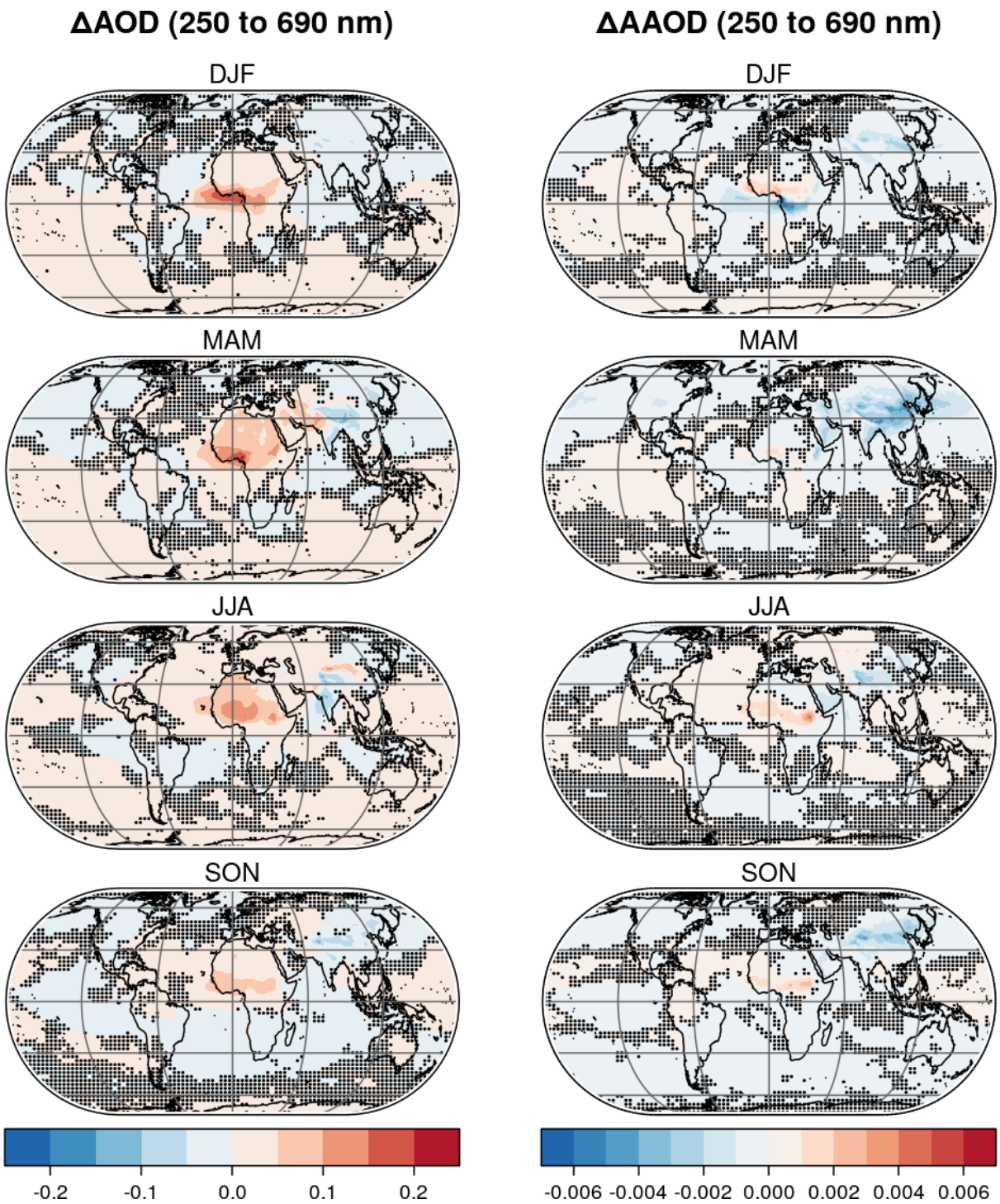

Figure S15: Same as Fig. 3, but for each season (December, January, February (DJF); March, April, May (MAM); June, July, August (JJA); September, October, November (SON)) individually.

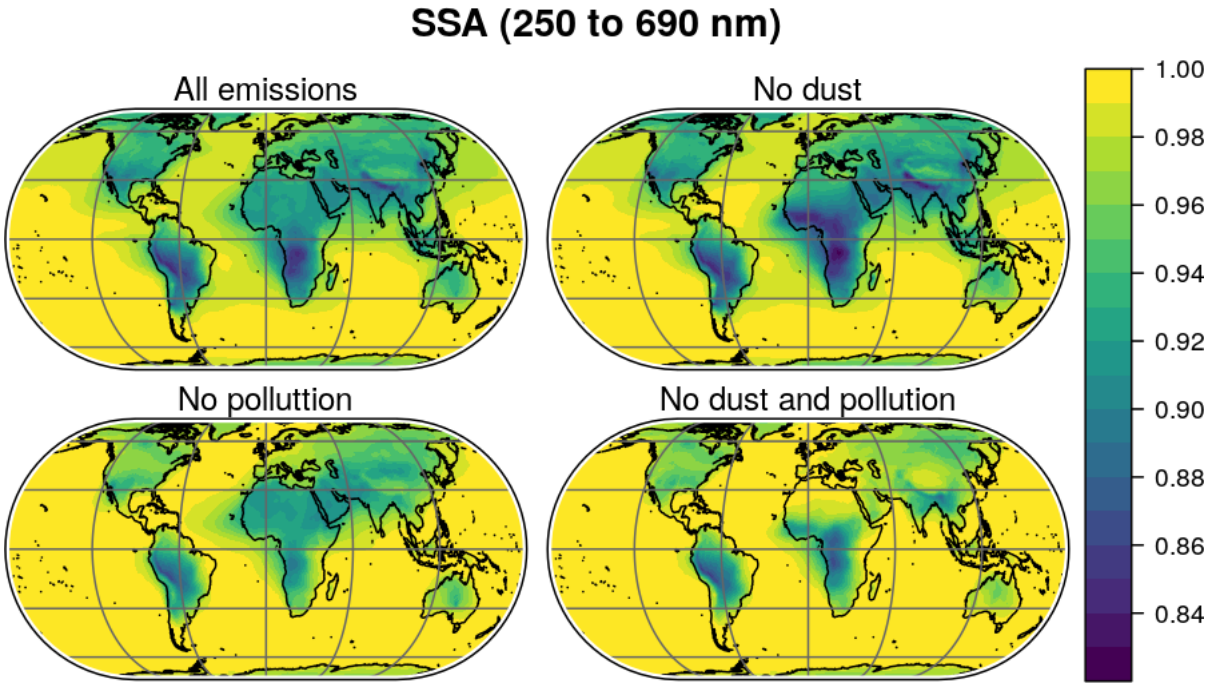

Figure S16: Annual mean of the extinction weighted single scattering albedo (SSA) for the different emission setups.

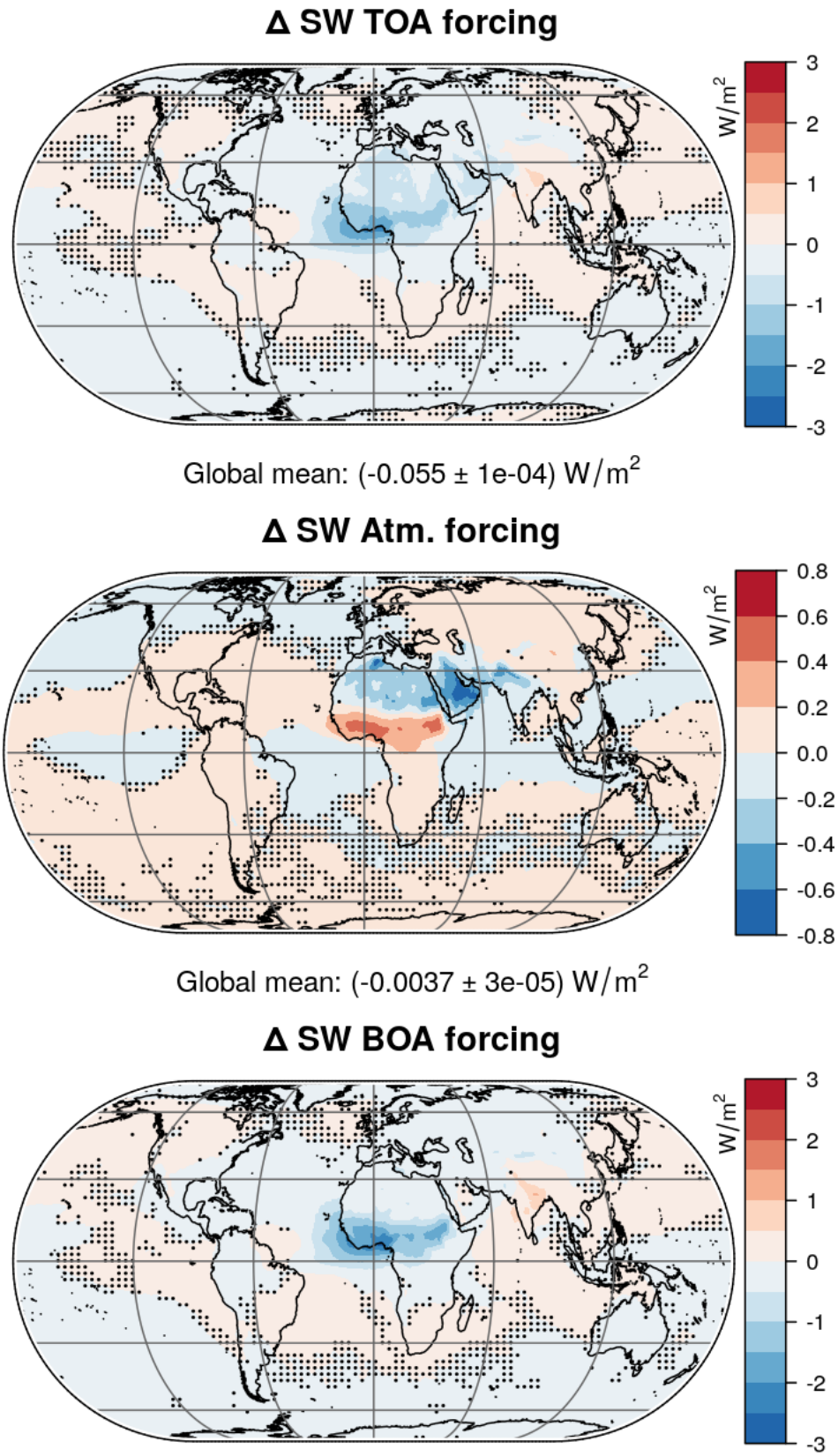

Figure S17: Same as Fig. 5, but only considering solar (shortwave, SW) radiation.

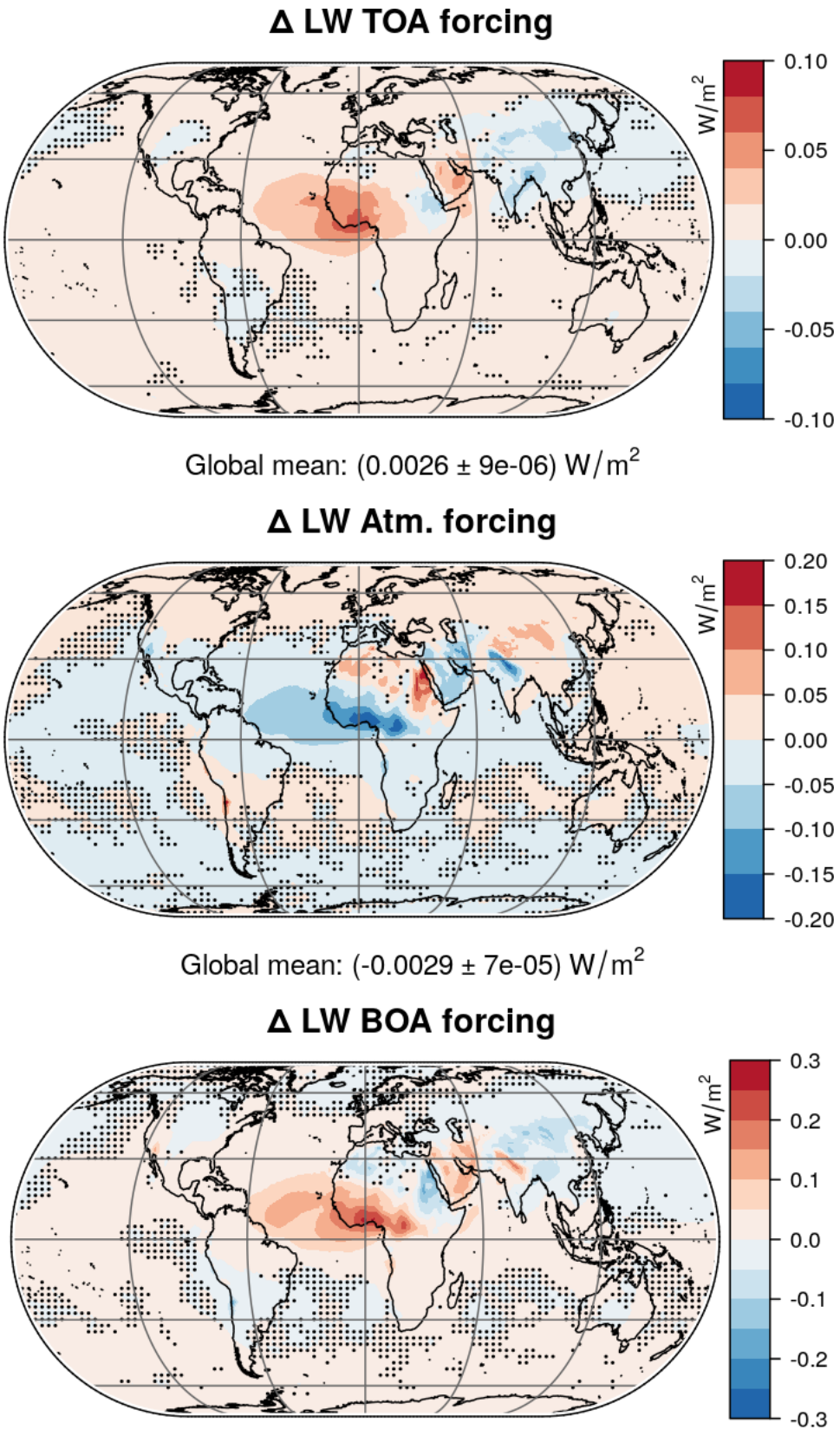

Figure S18: Same as Fig. 5, but only considering terrestrial (longwave, LW) radiation.

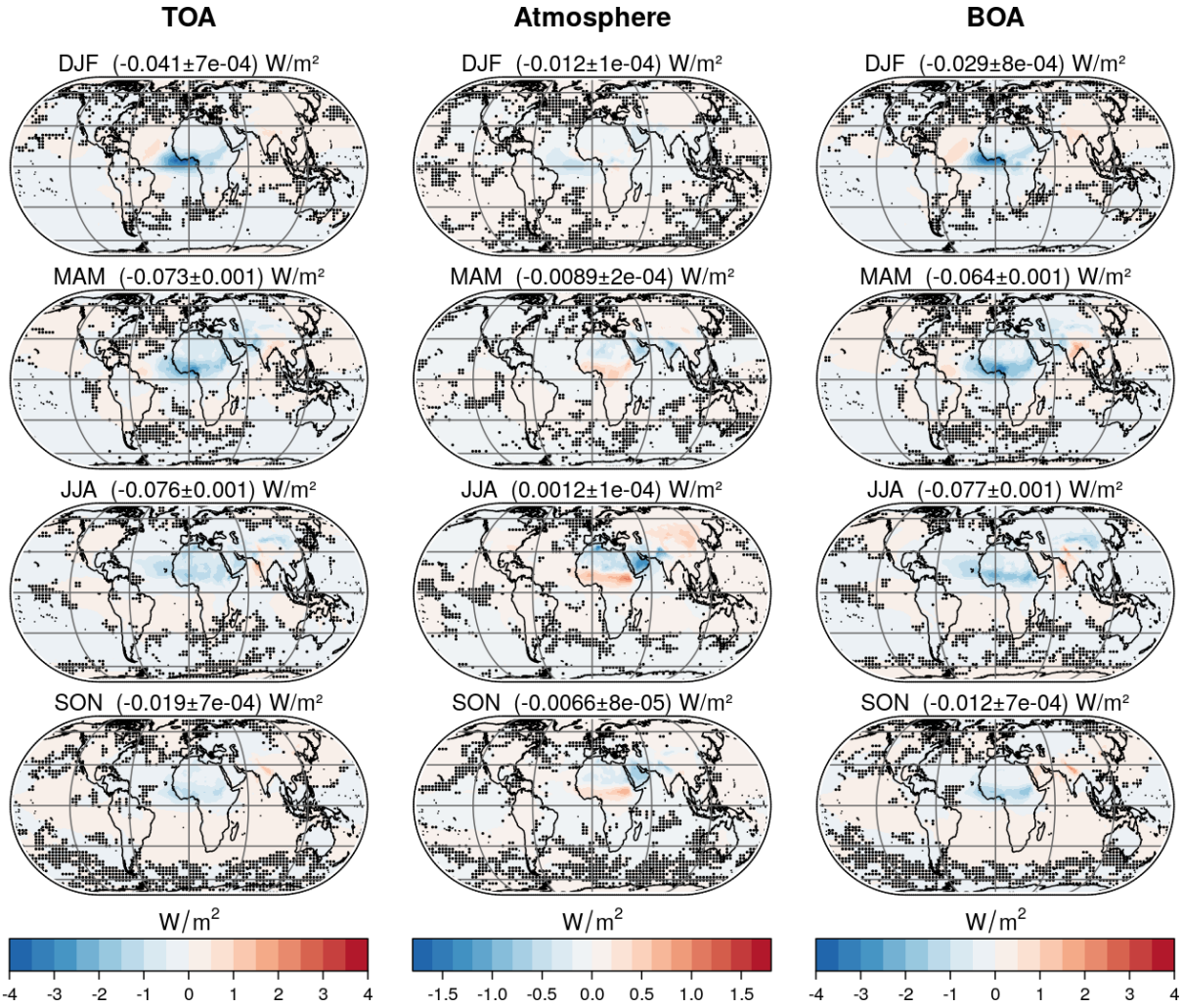

Figure S19: Same as Fig. 5, but for each season (December, January, February (DJF); March, April, May (MAM); June, July, August (JJA); September, October, November (SON)) individually.

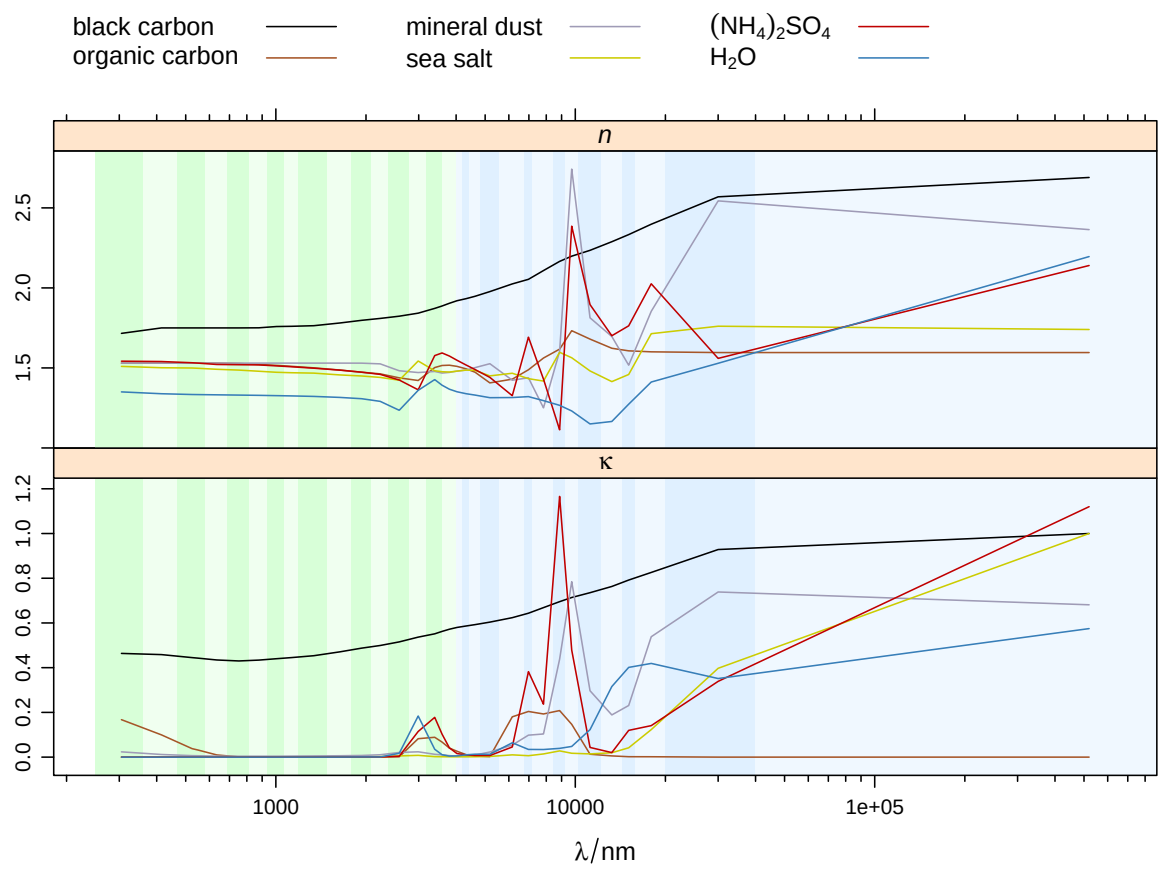

Figure S20: Real part n and imaginary part κ of refractive indices of various components used by the EMAC model. The data for ammonium sulphate ($(NH_4)_2SO_4$) also serves as default for other components. The background shading represents the shortwave (green, including the AEROPT sub-bands) and longwave (blue) bands used in EMAC. Adopted from the supplement of (Klingmüller et al. 2014).

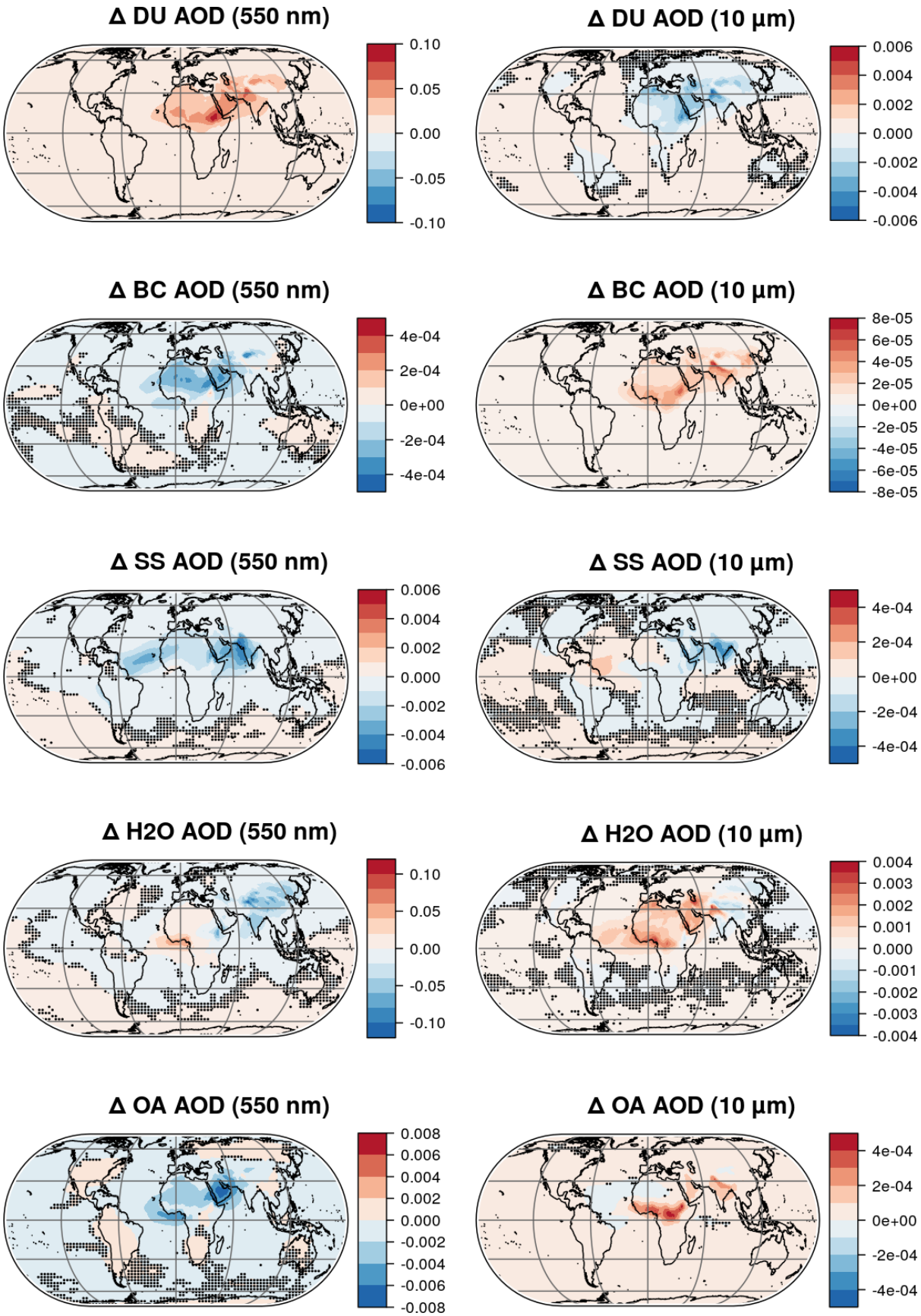

Figure S21: Effect of the dust-pollution interactions on the AOD contributions of (from top to bottom) bulk dust (DU), black carbon (BC), bulk sea salt (SS), water (H2O) and primary and secondary organic aersols including organic carbon (OA), at 550 nm (left column) and 10 μm (right column) wavelength.

Table S1: Real part n of the refractive indices displayed in Fig. S20 for the shortwave (top) and longwave (bottom) bands.

λ/μm	n					
	BC	OC	Dust	SS	$(NH_4)_2SO_4$	H_2O
0.25 – 0.36	1.72	1.53	1.53	1.51	1.54	1.35
0.36 – 0.47	1.75	1.53	1.53	1.50	1.54	1.34
0.47 – 0.58	1.75	1.53	1.53	1.50	1.53	1.33
0.58 – 0.69	1.75	1.53	1.53	1.49	1.52	1.33
0.69 – 0.81	1.75	1.53	1.53	1.49	1.52	1.33
0.81 – 0.94	1.75	1.52	1.53	1.48	1.52	1.33
0.94 – 1.06	1.76	1.52	1.53	1.47	1.51	1.33
1.06 – 1.19	1.76	1.51	1.53	1.47	1.51	1.33
1.19 – 1.49	1.76	1.50	1.53	1.47	1.50	1.32
1.49 – 1.78	1.78	1.49	1.53	1.46	1.49	1.32
1.78 – 2.08	1.80	1.47	1.53	1.45	1.47	1.31
2.08 – 2.38	1.81	1.46	1.53	1.44	1.46	1.29
2.38 – 2.78	1.82	1.44	1.48	1.42	1.42	1.24
2.78 – 3.19	1.84	1.42	1.47	1.54	1.36	1.36
3.19 – 3.59	1.87	1.50	1.48	1.48	1.58	1.43
3.59 – 4.00	1.90	1.52	1.47	1.47	1.57	1.37
3.3 – 3.8	1.89	1.52	1.47	1.48	1.59	1.39
3.8 – 4.2	1.92	1.51	1.48	1.48	1.55	1.35
4.2 – 4.4	1.93	1.49	1.49	1.49	1.52	1.34
4.4 – 4.8	1.95	1.47	1.50	1.48	1.49	1.33
4.8 – 5.6	1.98	1.41	1.53	1.45	1.44	1.31
5.6 – 6.8	2.02	1.43	1.42	1.47	1.33	1.31
6.8 – 7.2	2.05	1.49	1.44	1.43	1.69	1.32
7.2 – 8.5	2.11	1.56	1.25	1.42	1.43	1.30
8.5 – 9.3	2.17	1.62	1.60	1.60	1.11	1.27
9.3 – 10.2	2.20	1.73	2.74	1.56	2.39	1.23
10.2 – 12.2	2.23	1.68	1.81	1.48	1.90	1.15
12.2 – 14.3	2.29	1.62	1.70	1.41	1.70	1.17
14.3 – 15.9	2.33	1.61	1.52	1.46	1.76	1.27
15.9 – 20.0	2.40	1.60	1.85	1.71	2.03	1.41
20.0 – 40.0	2.57	1.60	2.54	1.76	1.56	1.53
40.0 – 1000.0	2.69	1.60	2.36	1.74	2.14	2.20

Table S2: Imaginary part κ of the refractive indices displayed in Fig. S20 for the shortwave (top) and longwave (bottom) bands.

λ/μm	κ					
	BC	OC	Dust	SS	$(NH_4)_2SO_4$	H_2O
0.25 – 0.36	0.46	0.17	0.024	2.1e-06	1.0e-07	1.7e-08
0.36 – 0.47	0.46	0.099	0.012	7.0e-08	1.0e-07	2.4e-09
0.47 – 0.58	0.44	0.038	0.0066	1.4e-08	1.0e-07	2.1e-09
0.58 – 0.69	0.43	0.0098	0.0045	3.8e-08	1.0e-07	1.7e-08
0.69 – 0.81	0.43	0.00099	0.0040	1.1e-06	1.2e-07	1.4e-07
0.81 – 0.94	0.43	0.00086	0.0040	2.8e-05	3.6e-07	8.1e-07
0.94 – 1.06	0.44	0.00077	0.0041	0.00014	1.3e-06	3.1e-06
1.06 – 1.19	0.45	0.00067	0.0045	0.00026	6.1e-06	1.3e-05
1.19 – 1.49	0.45	0.00051	0.0052	0.00043	3.1e-05	5.0e-05
1.49 – 1.78	0.47	0.00028	0.0061	0.00068	7.6e-05	1.0e-04
1.78 – 2.08	0.49	6.3e-05	0.0074	0.00097	0.00065	0.00069
2.08 – 2.38	0.50	8.2e-05	0.011	0.0020	0.0010	0.00068
2.38 – 2.78	0.52	0.0014	0.021	0.0053	0.0040	0.017
2.78 – 3.19	0.54	0.082	0.024	0.0079	0.11	0.18
3.19 – 3.59	0.55	0.089	0.013	0.0021	0.18	0.035
3.59 – 4.00	0.57	0.040	0.0067	0.0014	0.042	0.0045
3.3 – 3.8	0.56	0.067	0.010	0.0016	0.10	0.011
3.8 – 4.2	0.58	0.026	0.0044	0.0014	0.016	0.0055
4.2 – 4.4	0.59	0.011	0.0054	0.0014	0.0097	0.010
4.4 – 4.8	0.59	0.0050	0.0092	0.0017	0.0072	0.013
4.8 – 5.6	0.60	0.0022	0.023	0.0029	0.0072	0.013
5.6 – 6.8	0.62	0.18	0.054	0.010	0.045	0.064
6.8 – 7.2	0.64	0.20	0.098	0.0064	0.38	0.034
7.2 – 8.5	0.67	0.19	0.10	0.014	0.24	0.034
8.5 – 9.3	0.70	0.21	0.44	0.028	1.2	0.039
9.3 – 10.2	0.71	0.15	0.78	0.017	0.48	0.048
10.2 – 12.2	0.74	0.013	0.30	0.014	0.043	0.12
12.2 – 14.3	0.76	0.0054	0.19	0.019	0.020	0.32
14.3 – 15.9	0.79	0.0018	0.23	0.042	0.12	0.40
15.9 – 20.0	0.83	0.0016	0.54	0.12	0.14	0.42
20.0 – 40.0	0.93	0	0.74	0.40	0.34	0.35
40.0 – 1000.0	1.0	0	0.68	1.0	1.1	0.57

References

Bangalath, Hamza Kunhu, and Georgiy Stenchikov. 2015. "Role of Dust Direct Radiative Effect on the Tropical Rain Belt over Middle East and North Africa: A High-Resolution AGCM Study." *Journal of Geophysical Research: Atmospheres* 120 (May): 4564–84. doi:10.1002/2015JD023122.

Jacobson, Mark Z. 2001. "Global Direct Radiative Forcing Due to Multicomponent Anthropogenic and Natural Aerosols." *Journal of Geophysical Research: Atmospheres* 106 (D2): 1551–68. doi:10.1029/2000JD900514.

Klingmüller, K., B. Steil, C. Brühl, H. Tost, and J. Lelieveld. 2014. "Sensitivity of Aerosol Radiative Effects to Different Mixing Assumptions in the AEROPT 1.0 Submodel of the EMAC Atmospheric-Chemistry–Climate Model." *Geoscientific Model Development* 7 (5): 2503–16. doi:10.5194/gmd-7-2503-2014.

Liao, H., and J. H. Seinfeld. 1998. "Radiative Forcing by Mineral Dust Aerosols: Sensitivity to Key Variables." *Journal of Geophysical Research: Atmospheres* 103 (D24): 31637–45. doi:10.1029/1998JD200036.

Miller, R. L., and I. Tegen. 1998. "Climate Response to Soil Dust Aerosols." *Journal of Climate* 11 (12): 3247–67. doi:10.1175/1520-0442(1998)011<3247:CRTSDA>2.0.CO;2.

Miller, R. L., I. Tegen, and Jan Perlwitz. 2004. "Surface Radiative Forcing by Soil Dust Aerosols and the Hydrologic Cycle." *Journal of Geophysical Research: Atmospheres* 109 (February): D04203. doi:10.1029/2003JD004085.

Myhre, Gunnar, and Frode Stordal. 2001. "Global Sensitivity Experiments of the Radiative Forcing Due to Mineral Aerosols." *Journal of Geophysical Research: Atmospheres* 106 (D16): 18193–18204. doi:10.1029/2000JD900536.

Perlwitz, Jan, Ina Tegen, and Ron L. Miller. 2001. "Interactive Soil Dust Aerosol Model in the GISS GCM: 1. Sensitivity of the Soil Dust Cycle to Radiative Properties of Soil Dust Aerosols." *Journal of Geophysical Research: Atmospheres* 106 (D16): 18167–92. doi:10.1029/2000JD900668.

Reddy, M. Shekar, Olivier Boucher, Nicolas Bellouin, Michael Schulz, Yves Balkanski, Jean-Louis Dufresne, and Mai Pham. 2005. "Estimates of Global Multicomponent Aerosol Optical Depth and Direct Radiative Perturbation in the Laboratoire de Météorologie Dynamique General Circulation Model." *Journal of Geophysical Research: Atmospheres* 110 (May): D10S16. doi:10.1029/2004JD004757.

Shell, Karen M., and Richard C. J. Somerville. 2007. "Direct Radiative Effect of Mineral Dust and Volcanic Aerosols in a Simple Aerosol Climate Model." *Journal of Geophysical Research: Atmospheres* 112 (February): D03205. doi:10.1029/2006JD007197.

Tanaka, Taichu Y., Teruo Aoki, Hiroshi Takahashi, Kiyotaka Shibata, Akihiro Uchiyama, and Masao Mikami. 2007. "Study of the Sensitivity of Optical Properties of Mineral Dust to the Direct Aerosol Radiative Perturbation Using a Global Aerosol Transport Model." *SOLA* 3 (January): 33–36. doi:10.2151/sola.2007-009.

Woodward, S. 2001. "Modeling the Atmospheric Life Cycle and Radiative Impact of Mineral Dust in the Hadley Centre Climate Model." *Journal of Geophysical Research: Atmospheres* 106 (D16): 18155–66. doi:10.1029/2000JD900795.

Yoshioka, Masaru, Natalie M. Mahowald, Andrew J. Conley, William D. Collins, David W. Fillmore, Charles S. Zender, and Dani B. Coleman. 1970. "Impact of Desert Dust Radiative Forcing on Sahel Precipitation: Relative Importance of Dust Compared to Sea Surface Temperature Variations, Vegetation Changes, and Greenhouse Gas Warming." *Journal of Climate* 20 (January): 1445. doi:10.1175/JCLI4056.1.

Yue, Xu, Huijun Wang, Hong Liao, and Ke Fan. 2010. "Direct Climatic Effect of Dust Aerosol in the NCAR Community Atmosphere Model Version 3 (CAM3)." *Advances in Atmospheric Sciences* 27 (March): 230–42. doi:10.1007/s00376-009-8170-z.